Switching Pathways for Reversible Ligand Photodissociation in Ru(II) Polypyridyl Complexes with Steric Effects

Unjaroen, Duenpen; Chen, Juan; Otten, Edwin; Browne, Wesley R.

Published in:
Inorganic Chemistry

DOI:
10.1021/acs.inorgchem.6b02521

Inorganic Chemistry

Article

pubs.acs.org/IC

Switching Pathways for Reversible Ligand Photodissociation in Ru(II) Polypyridyl Complexes with Steric Effects

Duenpen Unjaroen, Juan Chen, Edwin Otten, and Wesley R. Browne*

Molecular Inorganic Chemistry, Stratingh Institute for Chemistry, University of Groningen, Nijenborgh 4, 9747 AG Groningen, The Netherlands

Supporting Information

ABSTRACT: The effect of a minor difference in ligand structure is shown to have a large effect on the photochemical pathways followed by two ruthenium(II) polypyridyl based complexes $[Ru(CH_3CN)\ (LL)]^{2+}$, **1** and **2**, where LL is MeN4Py (1,1-di(pyridin-2-yl)-*N*,*N*-bis(pyridin-2-yl-methyl)ethan-1-amine) or N4Py (1,1-di(pyridin-2-yl)-*N*,*N*-bis(pyridin-2-yl-methyl)-methanamine), respectively. In our earlier report we demonstrated near completely reversible two-way photochromism of **1**, in which a pyridyl ring dissociated on irradiation with visible light to form the thermally stable **1P**, $[Ru(CH_3CN)_2(MeN4Py)]^{2+}$. Complex **1** was recovered upon irradiation in the near-UV. Here, we show that the methyl group in the ligand backbone is critical to the reversibility by impeding the dissociation of one of the two sets of pyridyl rings. Irradiation of **2**, which does not bear the methyl group, with visible light results in formation of two thermally stable isomers **2a** and **2b**, which are characterized by UV−vis absorption, FTIR, ^{1}H NMR spectroscopy, ESI mass spectrometry, and X-ray crystallography. In contrast to **1P**, in both **2a** and **2b**, a different pyridyl moiety is dissociated. Whereas UV irradiation returns **2a** to its original state (**2**), the overall reversibility is limited by the relative stability of **2b**. The changes to the structure of **2** made possible by the increased freedom for all four pyridyl moieties to dissociate allows access to coordination modes that are not accessible thermally opening opportunities toward new catalysts for oxidation chemistry, photochromism and photoswitching.

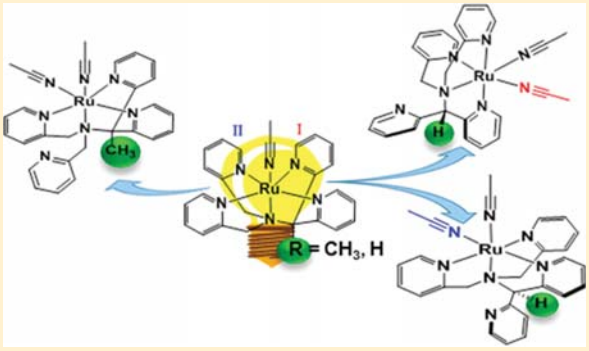

INTRODUCTION

Compounds that undergo well-defined and reversible structural changes following excitation with UV and visible light provide insight into the fundamental photophysical processes that occur in nature's photoswitching systems and are of increasing interest due to the wide range of applications that noninvasive control over molecular structure provides.[1] Over the last half century, organic photoswitches based on, primarily, light-induced pericyclic[2] and E/Z isomerization[3] reactions have seen widespread application in areas as diverse as materials science[4] and photochemical control of catalysis,[5] and biological activity.[6] More recently molecular photoswitching with transition metal complexes has emerged especially in the control of structure[7] and for selective small molecule release.[8] With the exception of hybrid inorganic−organic photoswitches,[9] transition metal based photochemistry is dominated by population of metal centered (dd) dissociative excited states, that is, promotion of electrons to antibonding metal−ligand orbitals.[10] Ruthenium(II) polypyridyl complexes are prominent in this field due to their remarkable photophysical and photochemical properties[11] including photoluminescence,[12] photoredox catalysis,[13] photoisomerization,[14] and photoinduced ligand exchange reactions.[15] The photochemistry of ruthenium(II) complexes is dominated by the lowest triplet metal-to-ligand charge transfer (^{3}MLCT)[16] and dissociative metal centered states,[17] and is typified by dissociative reactions in which excitation leads to partial or complete ligand dissociation followed by coordination of a new ligand or by a different donor atom on the ligand already present (linkage isomerism[18,19]). Thermally reversible ligand photodissociation has been reported by several groups, notably by Kojima,[20] and Sarkar and co-workers.[21] The selectivity of thermal and photochemical ligand dissociation in the complex $[Ru(TPA)(bpy)]^{2+}$ has been shown to be due to steric repulsion within the equatorial plane and has been explored extensively recently with density functional theory (DFT) methods.[21] In contrast to organic photochromes, such as dithienylethenes, photochemically induced changes in structure in inorganic complexes are typically either photochemically irreversible or the extent of reversibility is limited by the overlapping absorption spectra of each state.[19]

Recently, we reported the first example of a ruthenium(II) complex based on the pentadentate ligand **MeN4Py** [1,1-di(pyridin-2-yl)-*N*,*N*-bis(pyridin-2-yl-methyl)ethan-1-amine] in which near complete reversible two-way photoswitching (and photochromism) is observed. The reversible photochemical

Received: October 17, 2016
Published: January 3, 2017

DOI: 10.1021/acs.inorgchem.6b02521
Inorg. Chem. 2017, 56, 900−907

switching of $[Ru(CH_3CN)(MeN4Py)]^{2+}$ (**1**)[22] was achieved by irradiation with visible light to induce dissociation of a pyridine moiety, which was replaced by acetonitrile, to form the thermally stable complex **1P** as sole photoproduct.

The highly reversible photochemistry of **1** is remarkable, especially in regard to the selective dissociation of the least sterically encumbered '$-CH_2-$pyridyl's. The introduction of the methyl group in the synthesis of MeN4Py involves lithiation and subsequent methylation of N4Py (1,1-di-(pyridin-2-yl)-*N*,*N*-bis(pyridin-2-yl-methyl)methanamine) and hence the importance of the methyl group to the selectivity and especially reversibility of the photochromism of **1** prompted our study of its more easily prepared analogue $[Ru(CH_3CN)(N4Py)]^{2+}$ (**2**).

Here, we show that the photochromism of **2** involves dissociation of pyridyl moieties as observed for **1**, but is fundamentally different because of the absence of the methyl group. The photochemistry of **2** is shown, through a combination of UV−vis absorption, FTIR, ^{1}H NMR, spectroscopy, ESI mass spectrometry, and X-ray crystallography, to be dominated by dissociation of the more encumbered $-CH(pyridyl)_2$ moieties (i.e., bound to the tertiary carbon), leading to the reversible formation of two coordination isomers that are not accessible through thermal chemistry.

EXPERIMENTAL SECTION

Synthesis. All chemicals and solvents used in the synthesis were of analytical grade and used without further purification. Solvents for spectroscopic measurements were UVASOL (Merck) grade or better. The ligands 1,1-di(pyridin-2-yl)-*N*,*N*-bis(pyridin-2-yl-methyl)-methanamine (**N4Py**) is prepared according to the literature.[23] $[Ru(CH_3CN)(N4Py)](PF_6)_2$ (**2**) was prepared from $RuCl_3$ and N4Py via the $[Ru(Cl)(N4Py)]Cl$ complex (see Supporting Information for details) as described earlier for the analogous complex $[Ru(Cl)(MeN4Py)]Cl$.[22]

Physical Methods. UV−vis absorption spectra were recorded with a Specord600 (AnalytikJena) spectrophotometer in 1 cm path length quartz cuvettes. ^{1}H NMR spectra (400, 500, and 600 MHz) were recorded on a Varian Mercury Plus and Varian Inova, respectively. Chemical shifts are denoted relative to the residual solvent peak (^{1}H NMR spectra CD_3CN, 1.94 ppm). Elemental analyses were performed with a Foss-Heraeus CHN Rapid or a EuroVector Euro EA elemental analyzer. ESI mass spectra of complexes were recorded on a Triple Quadrupole LC/MS/MS mass spectrometer (API 3000, PerkinElmer Sciex Instruments). Raman spectra were recorded at λ_{exc} 785 nm using a PerkinElmer Raman Station at room temperature. FTIR spectra were recorded using a UATR (ZnSe) with a PerkinElmer Spectrum400, equipped with a liquid N_2 cooled MCT detector. Irradiation with UV−vis absorption detection was carried out at 355 nm (7 mW, Cobolt lasers), 457 nm (50 mW, Cobolt lasers). ^{1}H NMR spectroscopy with in situ irradiation at 420 nm (LED, M420F2, 10 mW at source, Thorlabs) and 365 nm (LED, M365FP1, 10 mW at source, Thorlabs) with light delivered via a 5 m (400 μm diameter) optical fiber in which the last 3 cm of cladding was removed and the bare fiber was lightly sanded to give an approximately uniform emission. The bare fiber end was inserted in the inner tube of a 5 mm Evan's NMR tube with the sample solution held in the outer compartment of the tube. NMR spectra were recorded during irradiation. As longer irradiation times were required than for irradiation of optically dilute solutions in 1 cm quartz cuvettes, full conversion to the photoproduct could not be achieved. Collection and analysis of X-ray diffraction data is described in the Supporting Information.

RESULTS

Structure and Spectroscopic Characterization of $[Ru(CH_3CN)(N4Py)](PF_6)_2$ (2). The ESI mass spectrum of **2** in acetonitrile shows a base peak at m/z 255.3 corresponding to the dication $[Ru(CH_3CN)(N4Py)]^{2+}$. The relative simplicity of the ^{1}H NMR spectrum of **2** in acetonitrile-d_3 reflects the plane of symmetry in the complex with two distinct sets of pyridyl signals and a singlet at 4.52 ppm assigned to the methylene signals (vide infra). The signal of the coordinated acetonitrile is at 2.74 ppm, confirming exchange of the chlorido ligand of the precursor $[Ru(Cl)(N4Py)]Cl$ for acetonitrile (vide infra). The UV−vis absorption spectrum of **2** in acetonitrile shows two absorption bands at 350 and 425 nm which are assigned to metal to ligand charge transfer (^{1}MLCT) transitions, respectively, (Figure 1a) similar to its analog $[Ru(CH_3CN)(MeN4Py)](BF_4)_2$ (**1**) (Figure S4a). Raman (λ_{exc} 785 nm) and IR spectra of **2** recorded in the solid state (Figures S8 and S9) show a C≡N stretch mode at 2276 cm^{-1} and pyridine modes in the region 1000−1600 cm^{-1}, which compare closely with those of $[Fe(CH_3CN)(N4Py)](ClO_4)_2$.[24]

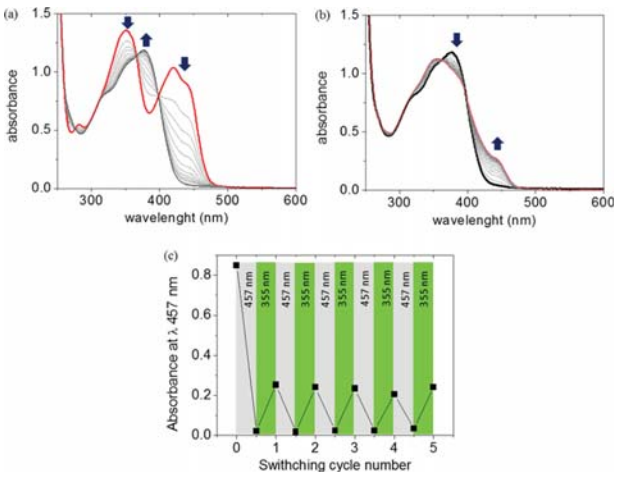

Figure 1. UV−vis absorption spectra of **2** (0.1 mM) (red) in acetonitrile (a) with irradiation at 457 nm, (b) with subsequent irradiation at 355 nm and (c) absorbance at 457 nm after sequential irradiation at 457 and 355 nm.

Photochemistry of 2. A complete loss in visible absorbance at 440 nm and a decrease in absorbance at 355 nm is observed, concomitant with the appearance of a new band at 376 nm, upon irradiation of **2** in CH_3CN at λ_{exc} 457 nm (Figure 1a). Isosbestic points are maintained at 366 and 398 nm. The changes to the spectrum are consistent with dissociation of a pyridine moiety from the Ru(II) center, together with coordination of solvent as observed earlier for **1**.[22] However, in contrast to **1**, the thermal reversion of the photoproduct to **2** does not occur even upon heating at 70 °C for an extended period of time. Subsequent irradiation at 355 nm lead to only a partial recovery of the initial spectrum of **2** (photostationary state, PSS ∼20%, Figure 1b). Repeated alternate irradiation between 457 and 355 nm (Figure 1c), was reversible indicating that the primary photoproducts exhibited photochromism also. The ESI mass spectrum of **2** in acetonitrile after irradiation at 457 nm shows a base peak at m/z 275.8, which corresponds to the dication $[Ru(CH_3CN)(CH_3CN)(N4Py)]^{2+}$, and no significant signals other than that of **2**. Notably, irradiation in acetonitrile-d_3 resulted in a base peak corresponding to $[Ru(CH_3CN)(CD_3CN)(N4Py)]^{2+}$ (m/z 277.2) in which the original bound CH_3CN was retained (Figure S13). Subsequent irradiation at 355 nm resulted in the

DOI: 10.1021/acs.inorgchem.6b02521
Inorg. Chem. 2017, 56, 900−907

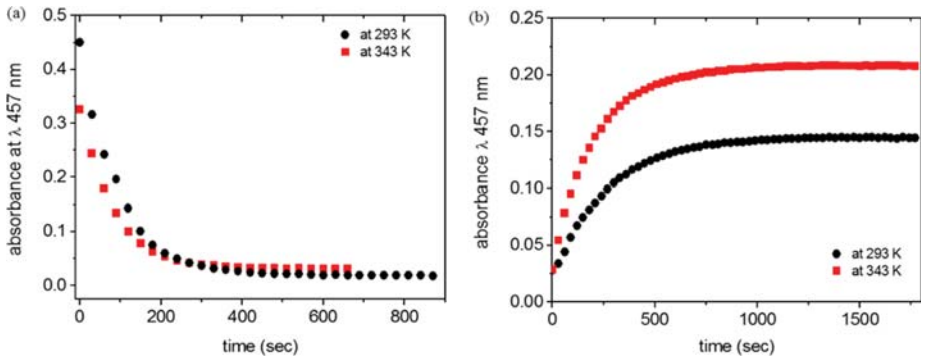

Figure 2. Change in absorbance of **2** in acetonitrile at 457 nm after irradiation at (a) 457 and (b) 355 nm at 293 and 343 K.

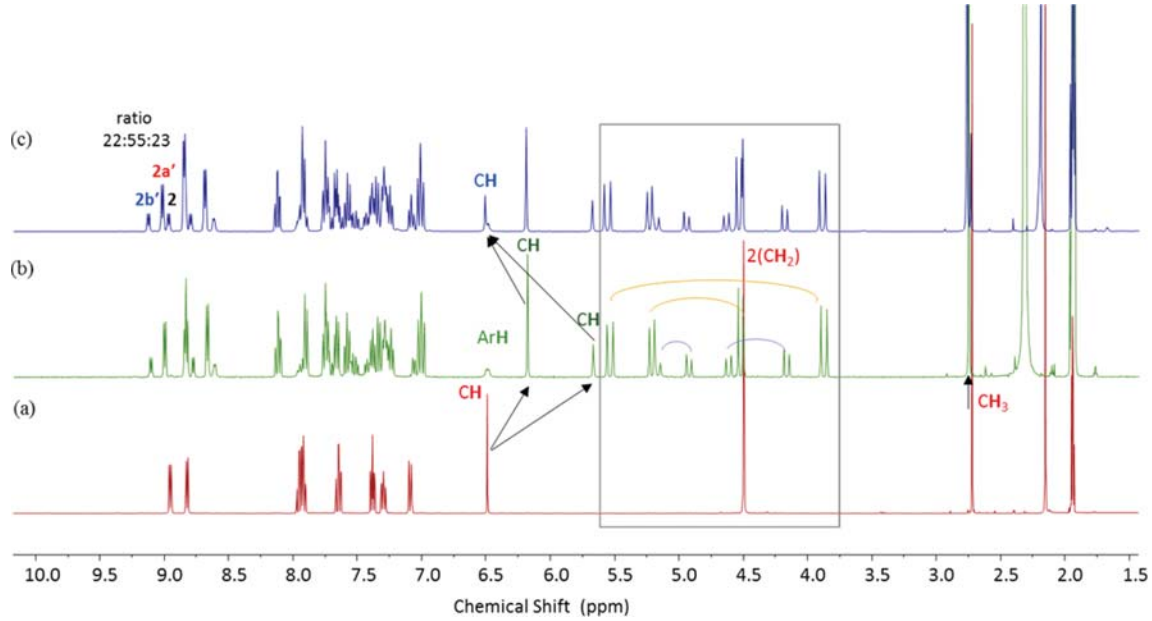

Figure 3. ^{1}H NMR spectrum of **2** in acetonitrile-d_3 (a) before and (b) after irradiation at 457 nm for 7 h and (c) after subsequent irradiation at 355 nm 18 h.

reappearance of the signal corresponding to $[Ru(CH_3CN)(N4Py)]^{2+}$ (**2**) at m/z 255.3. The photochemical quantum yields were determined by actinometry with ferrioxalate as a reference (Supporting Information). At 457 nm, the quantum yield for the conversion **2** to the mixture of products is 0.039, which is six-times greater than **1** (Φ = 0.0058).

Temperature Dependence of Photoswitching. As noted above, heating a solution of **2**, after it has reached PSS_{457nm}, to 343 K did not result in further spectral changes. Furthermore, the rate (and hence quantum yields) at which the PSS_{457nm} (a wavelength at which the photoproducts do not absorb) was reached was the same at 343 and 293 K indicating that this photochemical process is not thermally activated (Figure 2a). In contrast, irradiation at 355 nm, at 343 K, of a solution of **2** at PSS_{457nm} resulted in a 37% recovery of the initial spectrum of **2** compared with ~20% at room temperature (Figure 2b). Furthermore, the rate of recovery was greater at 343 K than at 293 K. These data indicate the photochemical reversion to the original state is thermally activated.

^{1}H NMR Spectral Analysis of Photoproducts. Although the changes observed for **2** upon irradiation at 457 nm are similar to those reported for **1**, the ^{1}H NMR spectrum of **2** in acetonitrile-d_3 after irradiation at 457 nm shows that a mixture of two complexes (**2a′** and **2b′**) with lower symmetry than **2** is obtained (Figure 3). The ratio of the major product (**2a′**) to the minor product (**2b′**) was 2:1, determined by integration of the signals of the coordinated acetonitrile ligands at 2.77 and 2.76 ppm, respectively. Subsequent irradiation of the $PSS_{457\ nm}$ mixture of **2a′** and **2b′** at 355 nm, at room temperature for 18 h, resulted in the partial recovery of **2** with a ratio of 23:55:22 for **2**:**2a′**:**2b′** (Figure 3c). The 4-fold increase in the number of resonances in the aromatic region and the appearance of doublets of the methylene protons (i.e., the CH_2 protons are both diastereotopic and are all inequivalent) observed reflects the decrease in symmetry, consistent with dissociation of only one pyridine moiety in each case. The singlet of the tertiary alkyl proton (CH) of **2** is shielded in the photochemical products moving from 6.49 to 6.19 ppm and 5.68 ppm for **2a′** and **2b′**, respectively (vide infra). The spectral assignment was carried out using a combination of NOESY, COSY, and HMBC NMR spectroscopy on the $PSS_{457\ nm}$ mixture, however, complete assignment of only the major product was achieved; the assignment of the spectrum of the minor product was precluded by the overlap of signals and low concentration

DOI: 10.1021/acs.inorgchem.6b02521
Inorg. Chem. 2017, 56, 900−907

(Figure S17–S22). Although the signals of **2a′** are temperature independent between 243 and 343 K, several of the signals of **2b′** are temperature dependent over this range (Figure S23). The broad singlet at 6.50 ppm assigned to a hydrogen of a pyridyl moiety of **2b′** narrowed with an increase in temperature from 298 to 348 K. At 243 K, the signals of the alkyl protons and some of the pyridyl signals of **2b′** broadened, consistent with hindered rotation of the unbound pyridyl ring. Overall, the spectral data indicated that for both **2a′** and **2b′**, one of pyridine moieties connected to tertiary alkyl carbon (CH) group was dissociated in contrast to the photochemistry observed for **1** in which one of the pyridyl moieties attached via a methylene unit is dissociated (Scheme 1).[22] The structural

Scheme 1. Reversible Photochemistry of $[Ru(CH_3CN)(MeN4Py)]^{2+}$ (1) upon Irradiation at 457 nm and Subsequently Irradiation at 355 nm[22]

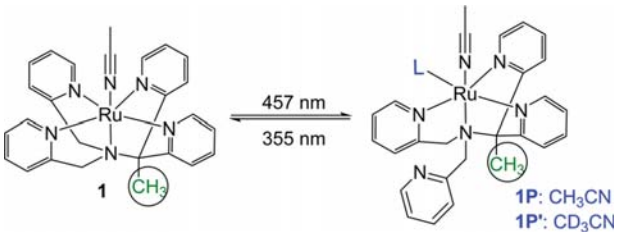

assignment of **2a′** and **2b′** was facilitated by isolation of crystals from the PSS_{457nm} mixture, with the structure of **2a′** confirmed unambiguously by X-ray crystallographic analysis (vide infra).

In situ irradiation at 420 nm of **2** and subsequently at 365 nm, with acquisition of ^{1}H NMR spectrum at 5 min intervals (Figure 4), showed that the loss and recovery of **2**, respectively,

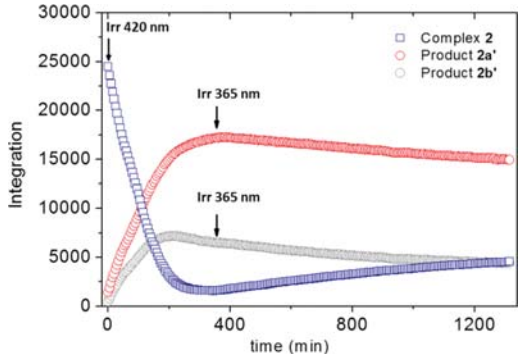

Figure 4. Intensity of pyridyl (H6) signals of **2**, **2a′**, and **2b′**, following irradiation of a solution of **2** at 420 nm and subsequent irradiation at 365 nm.

occurred without a change in the ratio of **2a′** and **2b′** (2:1), followed by the time dependence of the integral at δ = 9.13, 9.02, and 8.96 ppm, that is, a pyridine H6 signal of **2b′**, **2a′**, and **2**, respectively.

X-ray Structural Analysis. A single crystal of photoproduct **2a′** suitable for structural analysis by X-ray diffraction was obtained, from a solution of **2** at $PSS_{457\ nm}$. The Ru(II) ion in **2a′** is coordinated by four N atoms of the ligand N4Py (three pyridine N atoms and one amine N atom), one nitrogen atom from a CH_3CN molecule, and the sixth nitrogen from CD_3CN. The noncoordinated pyridine is connected to the tertiary alkyl carbon (CH) and two pyridines connected in the ligand via the methylene units are arranged cis to each other (Figure 5). The bond length between the central Ru(II) ion

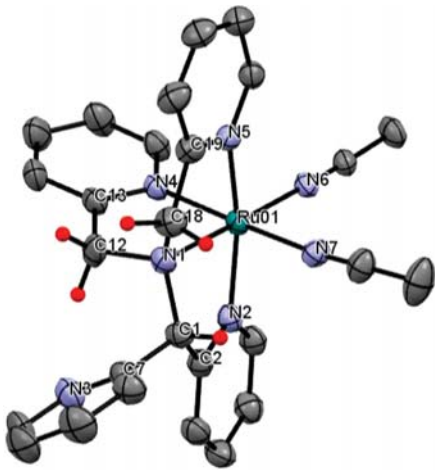

Figure 5. Perspective view of **2a′** $[Ru(CH_3CN)(CD_3CN)(N4Py)]^{2+}$. Ellipsoids are drawn at 50% probability level. Pyridyl and acetonitrile H atoms, counteranions, and solvent molecules are omitted for clarity. Selected bond lengths (Å): Ru–N1 = 2.067(3), Ru–N2 = 2.059(3), Ru–N4 = (2.044(3), Ru–N5 = 2.063(3), Ru–N6 = 2.035(3), Ru–N7 = 2.038(3). Selected bond angles (deg): N1–Ru01–N6 = 177.1(1), N4–Ru01–N7 = 175.2(1).

and the pyridine N atoms of N4Py are in the normal range and correspond to those in $[Ru(Cl)(N4py)]ClO_4{\cdot}CH_3OH$.[25] The $Ru–N1_{amine}$ bond (2.067 (3) Å) is longer than those reported for $[Ru(Cl)(N4Py)]ClO_4{\cdot}CH_3OH$ and $[Ru(OH_2)(N4Py)](PF_6)_2$[26] while the $Ru–N_{acn}$ (N6 and N7) bond lengths are shorter than the $Ru–N_{pyridine}$ (N2, N4, and N5) and $Ru–N_{amine}$ bonds. The short bond between Ru and N (acetonitrile) is consistent with reported ruthenium(II) nitrile bond lengths. The bond angle of N1–Ru1–N2 (81.4(1) Å), in which N1 is connected to the tertiary (C1) atom of N4Py is similar to those reported elsewhere (e.g., $[Ru(Cl)(N4Py)]ClO_4{\cdot}CH_3OH$).[25] Although single crystals of **2b′** were obtained also, the quality of the diffraction data set is rather poor and only serves to establish the atom connectivity. It is apparent from the data that **2b′** is an isomer in which the two Py-CH_2 moieties are coordinated in a trans arrangement with respect to each other (Scheme 2, Figure S25).

Photoreactivity of 2a′. Although efforts to separate **2a′** and **2b′** chromatographically were unsuccessful, isolation of **2a′** (in a 92:8 ratio of **2a′**/**2b′**) was achieved by fractional crystallization and allowed for the photochemistry of **2a′** to be explored in further detail. As observed for mixtures generated photochemically, the ratio of **2a′**/**2b′** was unaffected (determined by ^{1}H NMR spectroscopy) by heating in acetonitrile-d_3 at 70 °C for 2 h. By contrast, irradiation of a dilute solution at 355 nm resulted in a rapid change in the UV–vis absorption spectrum to that corresponding to a 2:1 ratio of **2a′** and **2b′**. Notably, irradiation of **2a′** at a more concentrated solution at 355 nm showed the formation of a mixture of **2**/**2a′**/**2b′** in the ratio of 52:38:10, by ^{1}H NMR spectroscopy, after 8 h, which confirms that the equilibrium between **2** and **2a′** is established more quickly than that between **2a′** and **2b′** (Figure 6). Hence, the conversion of **2a′** to **2b′** proceeds via **2** (vide infra).

DOI: 10.1021/acs.inorgchem.6b02521
Inorg. Chem. 2017, 56, 900–907

Scheme 2. Photoswitching of Coordination Mode in $[Ru(CH_3CN)(N4Py)]^{2+}$ (2) by Irradiation at 457 nm and Subsequent Irradiation at 355 nm[a]

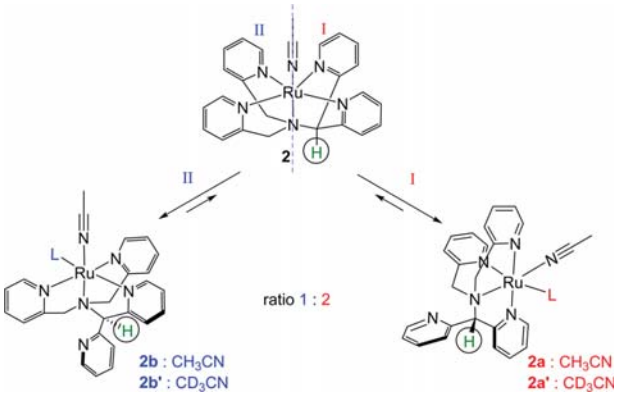

[a]Pathway **I** involves dissociation of pyridyl moieties attached to tertiary carbon (CH) to form **2*a*/2a′**, whereas pathway **II** involves the dissociation of pyridyl moieties attached via methylene units, followed by photoinduced rearrangement to form **2*b*/2b′**.

DISCUSSION

Complexes **2** and **1** are similar except for the replacement of a hydrogen with a methyl group in the ligand backbone (Scheme 1 and 2). In our early report[22] of the photochemistry of **1**, we demonstrated that irradiation at 457 nm resulted in the formation of **1P**, in which one of the pyridyl moieties connected to a secondary carbon (CH_2) undergoes dissociation exclusively (Scheme 1). In contrast to **1**, complex **2** forms a mixture of two products upon irradiation (Scheme 2). UV−vis absorption, ESI mass spectrometry, ^{1}H NMR spectroscopy experiments, and X-ray crystallography indicated that the photoproducts of **2** are isomers in which a tertiary pyridyl moiety is dissociated with a reduction in symmetry. The two photoproducts are thermally stable and are coordination isomers of each other each with an additional CH_3CN coordinated to the Ru(II) center (i.e., identical m/z). The photoproducts interconvert photochemically via **2** or a common intermediate, manifested in the preservation of isosbestic points during irradiation at low concentration, and the variation in the ratio of **2a′** and **2b′** observed only when isolated **2a′** was irradiated initially. The X-ray structures of the major product (**2a′**) shows that the $-CH_2-$pyridyls coordinate in a *cis* manner, whereas in the minor product (**2b′**) these pyridyl moieties are arranged trans to each other. The assignment is confirmed by the structural assignments made by 2-D NMR spectroscopy (Figure S17−S22).

There are two reasonable pathways to access each of the photoproducts (pathways **I** and **II** in Scheme 3), with both pathways involving sequential dissociation of pyridyl units. The major product **2a** can be generated (pathway **I**, Scheme 3) directly by dissociation of one of pyridyl units at the tertiary carbon with coordination of acetonitrile (specifically acetonitrile-d_3 in the case of **2a′**). The minor product **2b** cannot be generated by a common intermediate as irradiation of **2a′** leads first to conversion to **2** before the appearance of **2b**. Dissociation of a methylene bound pyridyl unit is followed by coordination of solvent (pathway **II**, Scheme 3). The noncoordinated pyridyl unit subsequently rotates and recoordinates to the Ru(II) center to form *trans*-**2b**. VT NMR experiments on the photoproducts confirm that **2a** and **2b** are not in thermal equilibrium.

^{1}H NMR spectral data confirmed that **2a′** and **2b′** form directly from **2** upon visible irradiation with a ratio of 2:1. This ratio is maintained upon subsequent photochemical reversion to **2** upon irradiation at 355 or 365 nm. The ^{1}H NMR spectrum of **2a′** (containing ca. 8% of **2b′**) after irradiation at 355 nm shows that complex **2** is recovered without an increase in the concentration of **2b′**. These data confirm that the two photoproducts do not interconvert with each other directly and that **2b′** is generated from **2** directly. Formation of **2b′** via **Ia** is unlikely given that irradiation of **2a′** does not lead immediately to **2b′**.

The importance of the methyl group of MeN4Py to the photochemistry of **1** observed is remarkable given that the electronic effects of such a group are expected to be minimal given the close similarity of the electronic and electrochemical properties of **1** and **2**. In the forward reaction, the steric effect (Thorpe−Ingold) of the methyl group appears to preclude dissociation of the $-C(CH_3)(-pyridyl)_2$ moieties (pathway **I**, Scheme 3), with only the $-CH_2-$pyridyl moieties undergoing dissociation and substitution by solvent (Scheme 1, it should be

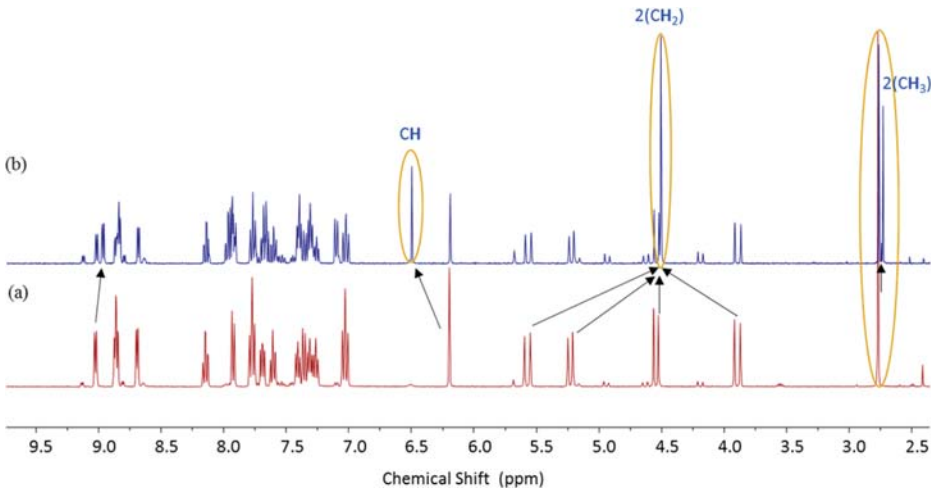

Figure 6. ^{1}H NMR spectrum of **2a′/2b′** (92:8) in acetonitrile-d_3 (a) before irradiation (b) after irradiation at 355 nm for 8 h.

DOI: 10.1021/acs.inorgchem.6b02521
Inorg. Chem. 2017, 56, 900−907

Scheme 3. Proposed Mechanism for the Reaction of 2 in Acetonitrile under Irradiation at 457 nm

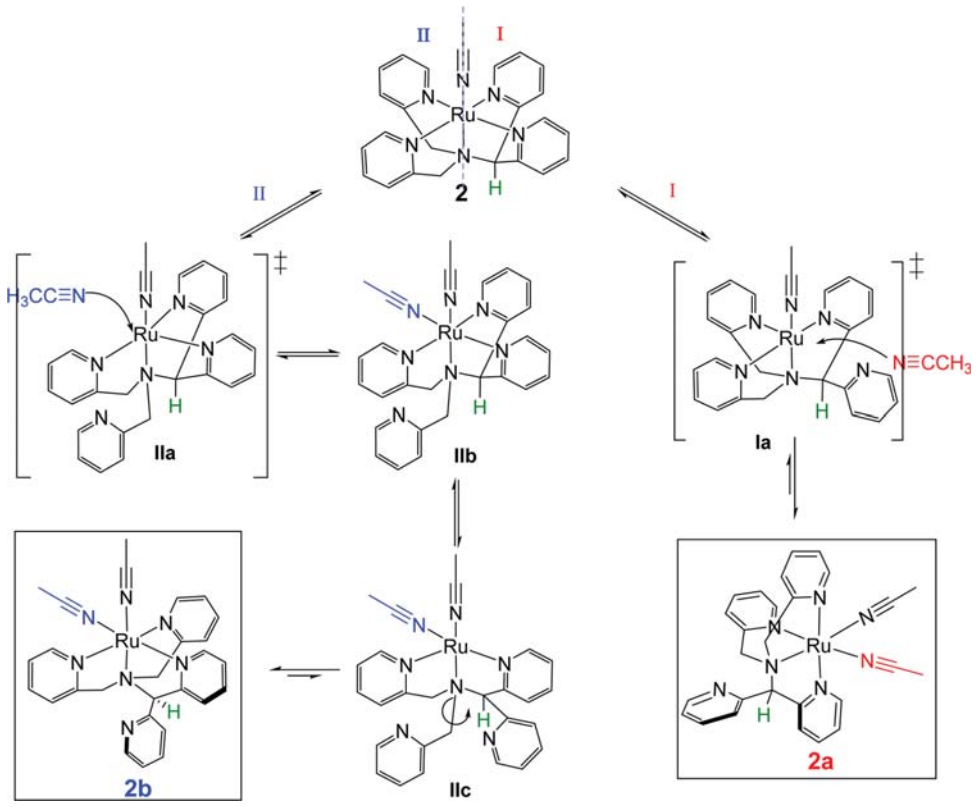

noted also that in the case of complex **1**, careful examination of the spectrum obtained[22] upon irradiation with visible light shows very weak signals that indicate that very minor amounts of complexes analogous to **2a**/**2b** are formed). In contrast, complex **2** is not subjected to such steric constraints and both types of pyridyl units can dissociate to form photoproducts. Hence, for **2** irradiation leads to both of photoproducts **2a** and **2b** and a photoproduct analogous to **1P** is not observed.

CONCLUSIONS

The steric repulsion of the methyl group on ligand MeN4Py is the main reason for the photoreactivity of **1** which diverges from that of **2**. The data presented here demonstrate that in the absence of a methyl group in the N4Py ligand photoinduced dissociation of pyridine units on both sides (pathway **I** and **II**, Scheme 3) can occur with the result that two thermally stable isomers are formed in which the pyridyl unit attached to −CH− moiety is no longer coordinated. The data indicate that these changes are reversible photochemically but not thermally.

Finally, the photochemistry of **2** provides access to novel species of Ru(II) polypyridyl complexes that are not accessible by thermal reactions. These photoproducts are expected to show distinct chemical reactivity especially in catalytic oxidations of organic compounds[27] and opens up new opportunities in the fields of photochromism, photo switching and oxidation catalysis.

ASSOCIATED CONTENT

Supporting Information

The Supporting Information is available free of charge on the ACS Publications website at DOI: 10.1021/acs.inorgchem.6b02521.

Details of experimental method and syntheses, spectroscopic, X-ray crystallographic data, and quantum yield determination (PDF)

Crystallographic information file for compound **2a** (CIF)

Crystallographic information file for compound **2b** (CIF)

AUTHOR INFORMATION

Corresponding Author

*E-mail: w.r.browne@rug.nl.

ORCID

Edwin Otten: 0000-0002-5905-5108

Wesley R. Browne: 0000-0001-5063-6961

Notes

The authors declare no competing financial interest.

ACKNOWLEDGMENTS

The European Research Council (StG, no. 279549, DU, W.R.B.) and funding from the Ministry of Education, Culture and Science (Gravity program 024.001.035, W.R.B.) are acknowledged for financial support. A. van Dam (ERIBA, University of Groningen) is thanked for assistance with a recording of ESI mass spectra. P. van der Meulen (University of Groningen) is thanked for assistance with a recording of 2D-NMR (600 MHz), VT NMR (500 MHz) spectra, and in situ irradiation with ^{1}H NMR spectroscopy.

DOI: 10.1021/acs.inorgchem.6b02521
Inorg. Chem. 2017, 56, 900−907

REFERENCES

(1) Feringa, B. L.; Browne, W. R. *Molecular Switches*; Wiley-VCH: Weinheim, Germany, 2011.

(2) (a) Irie, M. Diarylethenes for Memories and Switches. *Chem. Rev.* **2000**, *100*, 1685−1716. (b) Tian, H.; Yang, S. Recent Progresses on Diarylethene based Photochromic Switches. *Chem. Soc. Rev.* **2004**, *33*, 85−97.

(3) Feringa, B. L.; van Delden, R. A.; Koumura, N.; Geertsema, E. M. Chiroptical Molecular Switches. *Chem. Rev.* **2000**, *100*, 1789−1816.

(4) Russew, M. M.; Hecht, S. Photoswitches: From Molecules to Materials. *Adv. Mater.* **2010**, *22*, 3348−3360.

(5) (a) Wang, J.; Feringa, B. L. Dynamic Control of Chiral Space in a Catalytic Asymmetric Reaction Using a Molecular Motor. *Science* **2011**, *331*, 1429−1432. (b) Gostl, R.; Senf, A.; Hecht, S. Remote-controlling Chemical Reactions by Light: Towards Chemistry with High Spatio-temporal Resolution. *Chem. Soc. Rev.* **2014**, *43*, 1982−1996.

(6) (a) Szymański, W.; Beierle, J. M.; Kistemaker, H. A. V.; Velema, W. A.; Feringa, B. L. Reversible Photocontrol of Biological Systems by the Incorporation of Molecular Photoswitches. *Chem. Rev.* **2013**, *113*, 6114−6178. (b) Velema, W. A.; Szymanski, W.; Feringa, B. L. Photopharmacology: Beyond Proof of Principle. *J. Am. Chem. Soc.* **2014**, *136*, 2178−2191. (c) Szymanski, W.; Ourailidou, M. E.; Velema, W. A.; Dekker, F. J.; Feringa, B. L. Light-Controlled Histone Deacetylase (HDAC) Inhibitors: Towards Photopharmacological Chemotherapy. *Chem. - Eur. J.* **2015**, *21*, 16517−16524. (d) Lerch, M. M.; Hansen, M. J.; van Dam, G. M.; Szymanski, W.; Feringa, B. L. Emerging Targets in Photopharmacology. *Angew. Chem., Int. Ed.* **2016**, *55*, 10978−10999. (e) Broichhagen, J.; Frank, J. A.; Trauner, D. A Roadmap to Success in Photopharmacology. *Acc. Chem. Res.* **2015**, *48*, 1947−1960.

(7) (a) To, T. T.; Duke, C. B., III; Junker, C. S.; O'Brien, C. M.; Ross, C. R., II; Barnes, C. E.; Webster, C. E.; Burkey, T. J. Linkage Isomerization as a Mechanism for Photochromic Materials: Cyclopentadienylmanganese Tricarbonyl Derivatives with Chelatable Functional Groups. *Organometallics* **2008**, *27*, 289−296. (b) To, T. T.; Barnes, C. E.; Burkey, T. J. Bistable Photochromic Organometallics Based on Linkage Isomerization: Photochemistry of Dicarbonyl(η5-methylcyclopentadienyl)manganese(I) Derivatives with a Bifunctional, Nonchelating Ligand. *Organometallics* **2004**, *23*, 2708−2714.

(8) Vos, J. G.; Pryce, M. T. Photoinduced rearrangements in transition metal compounds. *Coord. Chem. Rev.* **2010**, *254*, 2519−2532.

(9) Harvey, E. C.; Feringa, B. L.; Vos, J. G.; Browne, W. R.; Pryce, M. T. Transition Metal Functionalized Photo- and Redox-Switchable Diarylethene based Molecular Switches. *Coord. Chem. Rev.* **2015**, *282-283*, 77−86.

(10) Tu, Y. J.; Mazumder, S.; Endicott, J. F.; Turro, C.; Kodanko, J. J.; Schlegel, H. B. Selective Photodissociation of Acetonitrile Ligands in Ruthenium Polypyridyl Complexes Studied by Density Functional Theory. *Inorg. Chem.* **2015**, *54*, 8003−8011.

(11) Sauvage, J. P.; Collin, J. P.; Chambron, J. C.; Guillerez, S.; Coudret, C.; Balzani, V.; Barigelletti, F.; De Cola, L.; Flamigni, L. Ruthenium(II) and Osmium(II) Bis(terpyridine) Complexes in Covalently-Linked Multicomponent Systems: Synthesis, Electrochemical Behavior, Absorption Spectra, and Photochemical and Photophysical Properties. *Chem. Rev.* **1994**, *94*, 993−1019.

(12) (a) Gill, M. R.; Thomas, J. A. Ruthenium(II) Polypyridyl Complexes and DNA—from Structural Probes to Cellular Imaging and Therapeutics. *Chem. Soc. Rev.* **2012**, *41*, 3179−3192. (b) Medlycott, E. A.; Hanan, G. S. Designing Tridentate Ligands for Ruthenium(II) Complexes with Prolonged Room Temperature Luminescence Lifetimes. *Chem. Soc. Rev.* **2005**, *34*, 133−142.

(13) (a) Nagib, D. A.; MacMillan, D. W. C. Trifluoromethylation of Arenes and Heteroarenes by Means of Photoredox Catalysis. *Nature* **2011**, *480*, 224−228. (b) Prier, C. K.; Rankic, D. A.; MacMillan, D. W. C. Visible Light Photoredox Catalysis with Transition Metal Complexes: Applications in Organic Synthesis. *Chem. Rev.* **2013**, *113*, 5322−5363. (c) Pham, P. V.; Nagib, D. A.; MacMillan, D. W. C. Photoredox Catalysis: A Mild, Operationally Simple Approach to the Synthesis of α-Trifluoromethyl Carbonyl Compounds. *Angew. Chem., Int. Ed.* **2011**, *50*, 6119−6122. (d) Tucker, J. W.; Stephenson, C. R. J. Shining Light on Photoredox Catalysis: Theory and Synthetic Applications. *J. Org. Chem.* **2012**, *77*, 1617−1622.

(14) (a) Yamazaki, H.; Hakamata, T.; Komi, M.; Yagi, M. Stoichiometric Photoisomerization of Mononuclear Ruthenium(II) Monoaquo Complexes Controlling Redox Properties and Water Oxidation Catalysis. *J. Am. Chem. Soc.* **2011**, *133*, 8846−8849. (b) Miyazaki, S.; Kojima, T.; Fukuzumi, S. Photochemical and Thermal Isomerization of a Ruthenium(II)-Alloxazine Complex Involving an Unusual Coordination Mode. *J. Am. Chem. Soc.* **2008**, *130*, 1556−1557. (c) Hirahara, M.; Ertem, M. Z.; Komi, M.; Yamazaki, H.; Cramer, C. J.; Yagi, M. Mechanisms of Photoisomerization and Water-Oxidation Catalysis of Mononuclear Ruthenium(II) Monoaquo Complexes. *Inorg. Chem.* **2013**, *52*, 6354−6364.

(15) (a) Bonnet, S.; Collin, J. P. Ruthenium-based light-driven molecular machine prototypes: synthesis and properties. *Chem. Soc. Rev.* **2008**, *37*, 1207−1217. (b) Liu, Y.; Turner, D. B.; Singh, T. N.; Angeles-Boza, A. M.; Chouai, A.; Dunbar, K. R.; Turro, C. Ultrafast Ligand Exchange: Detection of a Pentacoordinate Ru(II) Intermediate and Product Formation. *J. Am. Chem. Soc.* **2009**, *131*, 26−27. (c) Knoll, J. D.; Albani, B. A.; Turro, C. New Ru(II) Complexes for Dual Photoreactivity: Ligand Exchange and $^1O_2$ Generation. *Acc. Chem. Res.* **2015**, *48*, 2280−2287. (d) Scattergood, P. A.; Khushnood, U.; Tariq, A.; Cooke, D. J.; Rice, C. R.; Elliott, P. I. P. Photochemistry of $[Ru(pytz)\ (btz)_2]^{2+}$ and Characterization of a κ^1-btz Ligand-Loss Intermediate. *Inorg. Chem.* **2016**, *55*, 7787−7796.

(16) Hirahara, M.; Hakamata, T.; League, A. B.; Ertem, M. Z.; Takahashi, K.; Nagai, S.; Inaba, K.; Yamazaki, H.; Saito, K.; Yui, T.; Cramer, C. J.; Yagi, M. Mechanisms and Factors Controlling Photoisomerization Equilibria, Ligand Exchange, and Water Oxidation Catalysis Capabilities of Mononuclear Ruthenium(II) Complexes. *Eur. J. Inorg. Chem.* **2015**, *2015*, 3892−3903.

(17) Vos, J. G.; Kelly, J. M. Ruthenium Polypyridyl Chemistry; from Basic Research to Applications and Back Again. *Dalton Trans.* **2006**, 4869−4883.

(18) (a) McClure, B. A.; Rack, J. J. Two-Color Reversible Switching in a Photochromic Ruthenium Sulfoxide Complex. *Angew. Chem., Int. Ed.* **2009**, *48*, 8556−8558. (b) McClure, B. A.; Rack, J. J. Isomerization in Photochromic Ruthenium Sulfoxide Complexes. *Eur. J. Inorg. Chem.* **2010**, *2010*, 3895−3904.

(19) Fanni, S.; Weldon, F. M.; Hammarström, L.; Mukhtar, E.; Browne, W. R.; Keyes, T. E.; Vos, J. G. Photochemically Induced Isomerisation of Ruthenium Polypyridyl Complexes. *Eur. J. Inorg. Chem.* **2001**, *2001*, 529−534.

(20) Kojima, T.; Sakamoto, T.; Matsuda, Y. Toward a Photochemical and Thermal Molecular Machine: Reversible Ligand Dissociation and Binding in a Ruthenium(II)-2,2′-bipyridine Complex with Tris(2-pyridylmethyl)amine. *Inorg. Chem.* **2004**, *43*, 2243−2245.

(21) Weisser, F.; Plebst, S.; Hohloch, S.; van der Meer, M.; Manck, S.; Führer, F.; Radtke, V.; Leichnitz, D.; Sarkar, B. Tuning Ligand Effects and Probing the Inner-Workings of Bond Activation Steps: Generation of Ruthenium Complexes with Tailor-Made Properties. *Inorg. Chem.* **2015**, *54*, 4621−4635.

(22) Unjaroen, D.; Kasper, J. B.; Browne, W. R. Reversible Photochromic Switching in a Ru(II) Polypyridyl Complex. *Dalton Trans.* **2014**, *43*, 16974−16976.

(23) Lubben, M.; Meetsma, A.; Wilkinson, E. C.; Feringa, B. L.; Que, L., Jr. Nonheme Iron Centers in Oxygen Activation: Characterization of an Iron(III) Hydroperoxide Intermediate. *Angew. Chem., Int. Ed. Engl.* **1995**, *34*, 1512−1514.

(24) Draksharapu, A.; Li, Q.; Logtenberg, H.; van den Berg, T. A.; Meetsma, A.; Killeen, J. S.; Feringa, B. L.; Hage, R.; Roelfes, G.; Browne, W. R. Ligand Exchange and Spin State Equilibria of Fe^{II}(N4Py) and Related Complexes in Aqueous Media. *Inorg. Chem.* **2012**, *51*, 900−913.

(25) Kojima, T.; Weber, D. M.; Choma, C. T. {N-[Bis(2-pyridyl)methyl]-N,N-bis(2-pyridyl-methyl)amine-j5N}-

DOI: 10.1021/acs.inorgchem.6b02521
Inorg. Chem. 2017, 56, 900−907

chlororuthenium(II) Perchlorate Methanol Solvate. *Acta Crystallogr., Sect. E: Struct. Rep. Online* **2005**, *61*, m226−m228.
(26) Ohzu, S.; Ishizuka, T.; Hirai, Y.; Jiang, H.; Sakaguchi, M.; Ogura, T.; Fukuzumi, S.; Kojima, T. Mechanistic Insight into Catalytic Oxidations of Organic Compounds by Ruthenium(IV)-oxo Complexes with Pyridylamine Ligands. *Chem. Sci.* **2012**, *3*, 3421−3431.
(27) Yamaguchi, M.; Kousaka, H.; Izawa, S.; Ichii, Y.; Kumano, T.; Masui, D.; Yamagishi, T. Syntheses, Characterization, and Catalytic Ability in Alkane Oxygenation of Chloro(dimethyl sulfoxide)-ruthenium(II) Complexes with Tris(2-pyridylmethyl)amine and Its Derivatives. *Inorg. Chem.* **2006**, *45*, 8342−8354.

DOI: 10.1021/acs.inorgchem.6b02521
Inorg. Chem. 2017, 56, 900−907